

# Magnetization in the One-Dimensional Kondo Lattice

Shinji Watanabe

Department of Physics, Tohoku University, Sendai 980-8587

(July 28, 1999)

The magnetization curve in the one-dimensional Kondo lattice is calculated by the density matrix renormalization group method for the half-filled ( $n_c = 1$ ) and doped ( $n_c = 4=5$ ) cases. The stability of the intrasite f-c singlet brings about the magnetization plateau at  $1 - n_c$ , whose size is bounded by the spin gap  $\Delta_s$ . The abrupt increase of the magnetization is caused by the alignment of f spins around the magnetic field  $h_s$  and the collective Kondo singlet changes to the local triplets in the larger-h regime. In the process, the crossover from large to small Fermi surfaces for majority and minority spins is observed, whereas the Fermi surfaces are always contributed by f spin.

PACS numbers: 71.10.Fd, 75.30.Mb

In the heavy electron systems, the metamagnetism has been attracting great interest for a long time. The typical compound  $\text{CeRu}_2\text{Si}_2$  shows the metamagnetic behavior at the magnetic field  $H_M = 7.7 \text{ T}$  [1]. In the de Haas-van Alphen experiment, the size of the Fermi surface changes at  $H_M$  [2]. According to the band structure calculations [3], the measured Fermi surface is consistent with the itinerant f-electron band with the large Fermi surface below  $H_M$  and with the localized f electron with the small Fermi surface above  $H_M$ . So far, a number of analytical approaches and several numerical calculations [4-8] for the small clusters have been done. However, it has been still obscure how to understand the abrupt nonlinear increase of the magnetization accompanied with the change of the f-electronic character from the itinerant one to the localized one.

In this Letter, we clarify how the electronic state changes as the magnetic field increases by calculating the magnetization and the Fermi surfaces for the majority and the minority spins in the one-dimensional Kondo lattice model (KLM):

$$H = \sum_i \left( c_{i+1}^\dagger c_i + H \sigma_i^z \right) + J \sum_i S_i^f \cdot S_i^c \quad (1)$$

$$h \left( S_i^{fz} + S_i^{cz} \right);$$

where  $c_i^\dagger$  ( $c_i$ ) is the creation (annihilation) operator of the conduction electron on the  $i$ -th site ( $1 \leq i \leq L$ ) with spin  $\sigma$ .  $S_i^f$  and  $S_i^c$  are the spin operators on the  $i$ -th site of the f spin and the conduction electron, respectively. The rescaled magnetic field denoted by  $h$  includes the  $g$ -factor and the Bohr magneton  $\mu_B$ . The magnetization is defined by

$$m = n_{\uparrow}^f - n_{\downarrow}^f + n_{\uparrow}^c - n_{\downarrow}^c;$$

where  $n^f$  and  $n^c$  are the densities of the f spin and the conduction electron with spin  $\sigma$ , respectively.

We employ the density matrix renormalization group (DMRG) method [9] to study the magnetization process

of eq. (1) for both half-filled ( $n_c = n_{\uparrow}^c + n_{\downarrow}^c = 1$ ) and doped ( $n_c = 4=5$ ) cases. The procedure to obtain the magnetization curve is as follows: First, we set  $h = 0$  and calculate the lowest energy  $E(N_{\uparrow}; N_{\downarrow})$  of each subspace specified by  $N_{\uparrow} = L(1 + n_c + m)/2$  and  $N_{\downarrow} = L(1 + n_c - m)/2$ . Here  $n_c$  is fixed and  $m$  takes the range of  $0 \leq m \leq 1 + n_c$ . The magnetization is related to total  $S^z$  as  $m = 2S_{\text{tot}}^z/L$ . Then we obtain the magnetization  $m$  which minimizes the total energy of  $E(N_{\uparrow}; N_{\downarrow}) - hS_{\text{tot}}^z$  with respect to given  $h$ . In the DMRG calculation, we typically set the system size  $L = 40$  under the open boundary condition and the number of states kept is taken up to 300.

Figure 1 shows the magnetization curve and the local correlations under the magnetic field at half filling. As seen in Fig. 1(a), the magnetization appears beyond the threshold which is equal to the spin gap  $\Delta_s$  associated with the characteristic energy scale called Kondo temperature  $T_K$  at  $h = 0$  [10]. In order to illustrate the constituents of the magnetization, the average for the  $z$ -component of spin is shown in Fig. 1(b). It is clear that the main contribution to the rapid increase beyond  $\Delta_s$  stems from f spin, since  $hS_i^{fz}$  increases more rapidly than  $hS_i^{cz}$ . On the contrary, the property for the higher magnetic field up to the saturation  $h_s$  is characterized by the conduction electron; the divergent slope  $\partial m / \partial h \big|_{h_s} = 1$  comes from the divergent density of states at the band edge, which is intrinsic to the one-dimensional model [11]. In Fig. 1(c), the intra and intersite spin-spin correlations for the central  $i$ -th site are shown. At  $h = 0$ , the magnetic moments are mostly canceled by the antiferromagnetic array of f spins, and the residual moments are screened by formation of the collective Kondo singlet in the small- $J=t$  regime [5]. Even if  $h$  is switched on, the magnitude of the singlet correlations does not change as long as  $0 \leq h \leq \Delta_s$ . However, once  $h$  exceeds  $\Delta_s$ , the intersite antiferromagnetic correlation between f spins is destroyed abruptly to be the ferromagnetic one. On the contrary, the intrasite f-c singlet correlation remains until the larger magnetic field, and tends to the triplet gradually.

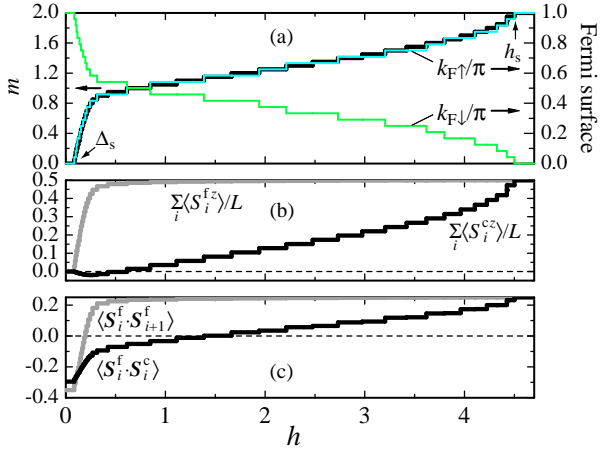


FIG. 1. (a) Magnetization curve and Fermi surfaces (b)  $\sum_i S_i^{fz}/L$  and  $\sum_i S_i^{cz}/L$  (c) intrasite correlation  $\sum_i S_i^f S_{i+1}^f$  and intersite correlation  $\sum_i S_i^f S_{i+1}^c$ , under the magnetic field  $h$  for  $t = 1$  and  $J = 1$  at  $n_c = 1$ .

We now turn to the location of the Fermi surface. Because of the spin-charge separation specific to one dimension, one cannot define the Fermi surface in the ordinary sense. In this paper we deduce the corresponding wave number  $k_F$  for each spin by a Friedel-type oscillation [13]. As shown in Ref. [14], the  $n$ -point correlation functions of the open boundary system are related to the  $2n$ -point functions of the periodic boundary system. Following Refs. [14,15], we have

$$\langle N^c(x) \rangle = A \frac{\cos(2k_F^+ x)}{x} + A \frac{\cos(2k_F^- x)}{x} + B \frac{\cos[2(k_F^+ + k_F^-)x]}{x}; \quad (2)$$

where  $\langle N^c(x) \rangle = \langle N^+(x) \rangle + \langle N^-(x) \rangle$  is the one-particle charge density function under the open boundary condition. The spin density  $\langle S^{cz}(x) \rangle = \langle N^+(x) \rangle - \langle N^-(x) \rangle = 2$  has the same form as  $\langle N^c(x) \rangle$ , but with different coefficients  $A$  and  $B$ . Since the charge density is always uniform (i.e.,  $\langle N_i^c \rangle = 1$  for every site) at half filling, we show  $\langle S_i^{cz} \rangle$  with the oscillating pattern in Fig. 2 I(a). The Fermi wave number is derived from the peak structure in the Fourier spectrum of  $\langle N_i^c \rangle$  and  $\langle S_i^{cz} \rangle$  for each magnetization  $m$  as in Fig. 2 II(a). The resultant  $k_F$  is shown in Fig. 1(a). For  $0 < h < h_s$ ,  $k_F^+$  ( $k_F^-$ ) remains  $0$  ( $\pi$ ). As  $h$  increases from  $h_s$  to  $h_s$ ,  $k_F^+$  ( $k_F^-$ ) changes from  $0$  ( $\pi$ ) to  $(0)$  ( $0$ ) continuously. Note that  $k_F^+ = \pi$  is seen to be just located on  $m = 1$ .

As for the gap, it has been reported that the quasi-particle gap remains under the finite magnetic field because the commensurate relation  $k_F^+ + k_F^- = \pi$  holds at half filling [7]. If the system has a wide insulating gap, the Fourier spectrum of eq. (2) does not have a sharp peak. However, as shown in Fig. 2 II(a), we cannot distinguish a tiny gap which may give rise to a rather sharp peak in the Fourier spectrum. We then calculated the

charge gap defined by  $\epsilon_c = E(N^+ + 1; N^- + 1) + E(N^+ - 1; N^- - 1) - 2E(N^+; N^-)$ , and concluded that for  $h > h_s$  a tiny gap does exist in consistency with Ref. [7].

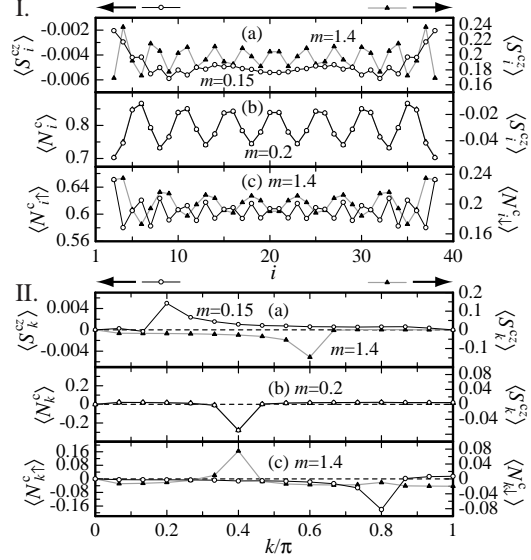


FIG. 2. One particle density in the real space (I) and its Fourier spectrum (II). (a)  $m = 0.15$  and  $m = 1.4$  for  $t = 1$  and  $J = 1$  at half filling. (b)  $m = 0.2$  and (c)  $m = 1.4$  for  $t = 1$  and  $J = 2$  at  $n_c = 4=5$ . The Fourier transformation is carried out by using the central 30 sites.

Let us consider the magnetization process for the doped case. Here we restrict to the paramagnetic metallic ground state without  $h$ , whereas a ferromagnetic metallic phase is known to exist in the large- $J=t$  regime [12]. Figure 3 shows the magnetization process for  $n_c = 4=5$ . A plateau appears with the magnitude of  $m = 1=5 = 1 - n_c$  as seen near the left end of Fig. 3 (a) (the enlargement will be given in Fig. 4). This can be intuitively understood if we take the real-space picture: The number  $L(1 - n_c)$  is equivalent to the number of the hole whose site has an only  $f$  spin. For  $0 < h < h_0$ , these  $f$  spins are polarized by the magnetic field, in order to avoid the energy loss to destroy the intrasite  $f$ - $c$  singlet correlation. As long as  $h_0 < h < h_1$ , this state is still stable so that the magnetization plateau appears. Once  $h$  exceeds  $h_1$ , the  $f$ - $c$  singlet starts to be destroyed and the situation becomes similar to the half-filled case for  $h > h_s$ . As seen in Figs. 3 (b) and 3 (c), the rapid increase of the magnetization is caused by the alignment of the  $f$  spins around  $h_1 < h < h_s$  and the collective Kondo singlet disappears gradually in the larger field.

As for the Fermi surface, it has been shown in the  $h = 0$  case that the Fermi wave number is given by  $k_F^+ = k_F^- = (1 + n_c)\pi = 9\pi = 10\pi$  [13]. Namely, the  $f$  spin contributes to the size of the Fermi surface at  $h = 0$ . To obtain  $k_F$  for  $h > 0$ , we calculate the one particle density and its Fourier spectrum as well as the half-filled

case. The case of  $m = 1=5$  which corresponds to the plateau is shown in Fig. 2 I(b). It turns out that the holes are located  $m$  usually keeping the interval of 4 sites. This con guration is also detected by the peak structure at  $2(k_{F\uparrow} + k_{F\downarrow}) = 2=5 \pmod{2}$  in Fig. 2 II(b), which persists in its position even if  $m$  changes. Additionally, there appears the  $2k_F$  peak for each spin whose position depends on  $m$ . As  $m$  increases ( $> 1$ ), the peak is detected more easily by  $\hbar n_i^c$  rather than by  $\hbar n_i^f$  and  $\hbar S_i^{cz}$ . We see that the clear two peaks of  $2k_{F\uparrow}$  and  $2k_{F\downarrow}$  appear and also that the amplitude for  $2(k_{F\uparrow} + k_{F\downarrow})$  becomes quite small in Fig. 2 II(c). We show the  $J = 2$  data in Figs. 2 (b) and 2 (c), since in the  $J = 1$  case the additional small peak which is not intrinsic appears as reported at  $h = 0$  [13]. The resultant  $k_F$  is shown in Fig. 3 (a). As  $h$  increases from 0 to  $h_0$ ,  $k_{F\uparrow}$  ( $k_{F\downarrow}$ ) increases (decreases) to  $(n_c = 4=5)$ , and they remain the same as long as  $h_0 < h < h_1$ . When  $h$  exceeds  $h_1$ ,  $k_{F\uparrow}$  increases from 0 and  $k_{F\downarrow}$  decreases from  $n_c$ . When  $h$  reaches the saturation field  $h_2 (< h_s)$ , we obtain  $k_{F\uparrow} = n_c = 4=5$  and  $k_{F\downarrow} = 0$ , which are equal to the Fermi surfaces of the completely polarized conduction bands decoupled to  $f$  spin. We conclude that  $n_c = 0$  for  $m = 1=5$  on which the plateau appears, and also for other  $m$ .

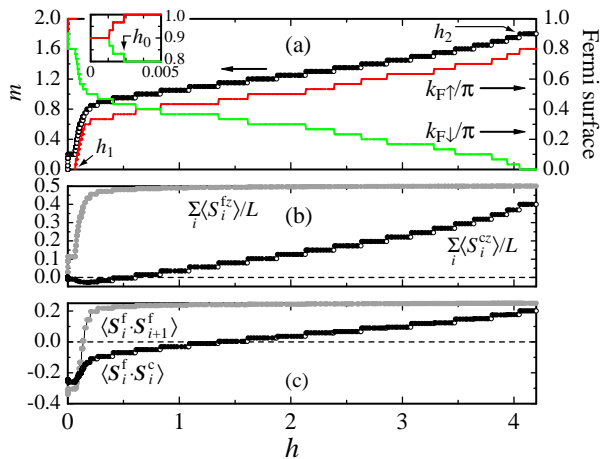


FIG. 3. (a) Magnetization curve and Fermi surfaces  $\hbar S_i^{fz}$  and  $\hbar S_i^{cz}$  (b) intrasite correlation  $\hbar S_i^f S_{i+1}^f$  and intersite correlation  $\hbar S_i^f S_{i+1}^c$ , under the magnetic field  $h$  for  $t = 1$  and  $J = 1$  at  $n_c = 4=5$ . The inset in (a) is the enlargement of the small  $h$  region for  $k_{F\uparrow}$  and  $k_{F\downarrow}$  (see text).

From the results for the  $n_c = 1$  and  $4/5$  cases, we conclude that the Fermi surfaces obtained with use of eq. (2) and the magnetization derived from the minimization of the total energy satisfy the following relation;  $k_F = (1 + n_c - m) = 2$ , where  $m$  ( $\#$ ) corresponds to  $+$  ( $-$ ) in the right hand side. This means that the Fermi surfaces are always large, which involve the contribution from  $f$  spin [16]. Our results obtained here are consistent with the argument on the basis of the generalized

Lieb-Schultz-Mattis theorem [17].

In order to analyze the crossover from large to small Fermi surface in detail, let us consider the periodic Anderson model (PAM):

$$H_{\text{PAM}} = \sum_i t \sum_{\langle i,j \rangle} c_{i+1}^\dagger c_i + H_{\text{sc}} + \sum_f \sum_i n_i^f + \sum_i V \sum_{\langle i,j \rangle} f_i^\dagger c_i + H_{\text{sc}} + U \sum_i n_i^f n_{i\#}^f \quad (3)$$

The KLM is the effective model derived from the PAM in the regime of  $U \gg V^2$  under the symmetric condition  $\mu_f + U = 2 = 0$ , where  $\mu_f$  is the density of states of the conduction electron at the Fermi energy. Finite  $U$  makes the effective  $f$  level shifted up to the Fermi energy where the Kondo resonance responsible for the heavy quasi-particle band arises. From the view point of the adiabatic continuation, we consider the simplest case of  $\mu_f = U = 2 = 0$  in eq. (3). In Fig. 4, we show the magnetization of the PAM with the Zeeman term  $h \sum_i (S_i^{fz} + S_i^{cz})$  for the doped ( $n = n_f + n_c = 9=5$ ) case.

For  $h_0 < h < h_1$  the plateau at  $m = 2$  appears as a consequence of the hybridization gap:  $\epsilon = 2t + 2t^2 + V^2$ . Here the critical fields  $h_i$  ( $i = 0; 1$ ) are given by

$$h_i = t \left( 1 - \cos(n) \right) \left( \frac{V}{\epsilon} \right) \frac{1}{1 + (V=t)^2} + \frac{V}{\cos^2(n) + (V=t)^2};$$

and the saturation field  $h_2$  by  $h_1 + t[1 + \cos(n)]$ . Namely, the plateau appears as long as the bottom of the upper empty band with majority spin becomes lower than the top of the lower filled band with minority spin as  $h$  increases. In order to separate the contribution from the conduction electron, we also show the magnetization for  $V = 0$ , setting  $n_f = 1$  and  $n_c = 4=5$ . Additionally, the data of  $J = 1$  and  $2$  in the KLM at  $n_c = 4=5$  are shown, whose horizontal axis is scaled by  $h_1$ . To facilitate the comparison between the PAM and the KLM, the magnetization curve of the PAM is also scaled by  $h_1$  and we choose the hybridization  $V$  fixing  $t = 1$  in eq. (3) so that  $h_1$  is equal to  $h_1$  of the KLM. The  $V = 0$  case is scaled by the same unit of the corresponding  $V \neq 0$  case. Before the discussion about the results, we should comment that the Fermi surface is related to the magnetization as  $k_F = (n - m) = 2$  in the PAM, which is written in the similar notation to the KLM case. Hence, one can directly switch from the magnetization curve to the Fermi surfaces in a magnetic field.

As for the PAM, we see in Fig. 4 that the magnetization for  $V \neq 0$  approaches that for  $V = 0$  with  $n_f = 1$  and  $n_c = 4=5$  as  $h$  increases. Namely, the crossover from  $f$  to conduction electron which gives the dominant contribution to the magnetization occurs in the larger magnetic field regime than  $h_1$ . For the large- $h$  region up to the saturation, the main contribution to the magnetization

as well as the Fermi surfaces comes from the conduction electron. Note that, even in this case, the f electron is coupled to the conduction electron; the f electron is always itinerant, but not localized. Since  $U$  is reduced to be the order of  $T_K = 2t \exp(-U/(8(0)V^2)g)$  by finite  $U$ , the range where the f electron gives the main contribution to the magnetization process will be drastically reduced by the many-body effects. As seen in the  $V \rightarrow 0$  limit, the Fermi surface can be close to that of the conduction electron beyond slightly larger  $h$  than  $h_1 = T_K$ , where the magnetization curve for  $V \neq 0$  becomes parallel to that for  $V = 0$ . This trend is increasingly visible as  $n$  approaches 2 (half filling). Namely, the crossover from large to small Fermi surfaces can be observed around the point indicated by the open arrow in Fig. 4, where the magnetic moment of f electron is not fully polarized.

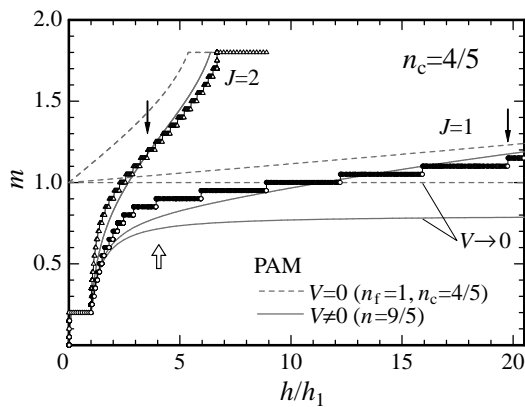


FIG. 4. Magnetization of the KLM for  $n_c = 4/5$  and of the PAM for  $n = 9/5$ , with  $t = 1$ . The dashed line represents the  $V = 0$  case of the PAM with  $n_f = 1$  and  $n_c = 4/5$ . Each data for  $V \neq 0$  and  $V = 0$  of the PAM is scaled by  $h_1$ , where  $h_1$  is set to be equal to  $h_1$  of the KLM. The solid arrows show the point where  $hS_1^f$  of the KLM changes the sign. The open arrow indicates the crossover point from large to small Fermi surfaces (see text).

The general behavior of the KLM is similar to that of the PAM. This implies that the real-space picture for the KLM explained in Fig. 3 connects with the  $k$ -space picture for the PAM continuously. As for the quantitative difference between them, the width of the plateau becomes narrower than  $h_s$  as  $n_c$  decreases from 1 in the KLM, whereas  $h_1 = h_0$  is always equal to in the  $U = 0$  PAM. As shown in Fig. 4, the magnetic field characterizing the coupling between f spin and conduction electron in the KLM is identified by the solid arrow on which the sign of  $hS_1^f$  changes (see Fig. 3(c)). In the case of the realistic parameter as  $J=t \neq 0$ , the location of the arrow will extend to the remarkably larger magnetic field than  $h_1 = T_K$ . However, we emphasize that similarly to the  $V \rightarrow 0$  limit of the PAM,  $k_F$  can be close to that of the conduction electron beyond slightly larger  $h$  than  $h_1 = T_K$  near half filling. Namely, the crossover from large to small Fermi surfaces can be observed around the

point such as the open arrow in Fig. 4, where the intrasite f-c singlet correlation remains.

To summarize, in the KLM the antiferromagnetic intersite correlation of f spins disappears rapidly around  $h_s$  and the collective Kondo singlet changes to the local triplets gradually in the larger magnetic field. In that process, the crossover from large to small Fermi surfaces is observed, whereas the Fermi surfaces are always contributed by f spin.

The author would like to thank H. Tsunetsugu, N. Shibata, H. Yamagami, M. Oshikawa, O. Sakai and Y. Kuramoto for valuable discussions. A part of the numerical calculation was performed by VPP500 at the Supercomputer Center of the ISSP, Univ. of Tokyo.

Electronic address: watanabe@cmpt01.phystohoku.ac.jp

- [1] J. M. Mignot, et al., J. Magn. & Magn. Mater. 76 & 77, 97 (1988); J. Rossat-Mignod, et al., J. Magn. & Magn. Mater. 76 & 77, 376 (1988);
- [2] H. Aoki, et al., Phys. Rev. Lett. 71, 2110 (1993); H. Aoki, et al., J. Phys. Soc. Jpn. 62, 3157 (1993).
- [3] H. Yamagami and A. Hasegawa, J. Phys. Soc. Jpn. 61, (1992) 2338; H. Yamagami and A. Hasegawa, J. Phys. Soc. Jpn. 62, (1993) 592.
- [4] K. Ueda, J. Phys. Soc. Jpn. 58, 3465 (1989).
- [5] K. Yamamoto and K. Ueda, J. Phys. Soc. Jpn. 59, 3284 (1990).
- [6] T. Saso and M. Ito, Phys. Rev. B 53, 6877 (1996).
- [7] H. M. Carruzzo and C. Yu, Phys. Rev. B 53, 15377 (1996).
- [8] K. Tsutsui, et al., Physica B 230-232, 421 (1997).
- [9] S. R. White, Phys. Rev. Lett. 69 2863 (1992); S. R. White, Phys. Rev. B 48, 10345 (1993).
- [10] H. Tsunetsugu, Y. Hatsugai and K. Ueda, Phys. Rev. B 46, 3175 (1992); N. Shibata, et al., Phys. Rev. B 53, R8828 (1996).
- [11] The lowest energy  $E$  for  $S_{\text{tot}}^z = L - 1$  at half filling is obtained by solving the self-consistent equation:  $E = \epsilon_0 - J^2/(4L) - \epsilon_q = (\epsilon_0 + \epsilon(q) - E)$ ; with  $\epsilon_0 = J(L-2)/4$  and  $\epsilon(q) = -4t \cos q$ , where  $q$  is the relative momentum. The saturation field is given by  $h_s = JL/4 - E$ .
- [12] H. Tsunetsugu, M. Sigrist and K. Ueda, Phys. Rev. B 47, 8345 (1993).
- [13] N. Shibata, et al., Phys. Rev. B 54, 13495 (1996); N. Shibata, A. Tsvelik and K. Ueda, Phys. Rev. B 55, 1 (1997).
- [14] J. L. Cardy, Nucl. Phys. B 240, 514 (1984).
- [15] G. Bedurfig, et al., Phys. Rev. B 58, 10225 (1998).
- [16] At the saturation with  $m = 1 + n_c$ , the Fermi surfaces can be equal to the small ones;  $2k_{F\#} = 2(1 + n_c) = 2n_c$  and  $2k_{F\#} = 0$ .
- [17] M. Yamana, M. Oshikawa and I. A. Aeck, Phys. Rev. Lett. 79, 1110 (1997).